ChemComm

COMMUNICATION

Simple bond patterns predict the stability of Diels–Alder adducts of empty fullerenes†

Paula Pla,[a] Yang Wang *[abc] and Manuel Alcamí *[abd]

Cite this: *Chem. Commun.*, 2018, **54**, 4156

Received 1st March 2018,
Accepted 27th March 2018

DOI: 10.1039/c8cc01709c

rsc.li/chemcomm

We present an extensive and systematic study on the regioselectivity of Diels–Alder (DA) cycloadditions to empty fullerenes, covering the whole range of cage sizes from C_{60} to C_{180}. Reaction energies obtained from DFT calculations, which correlate with activation barriers, can be well reproduced by using a simple Hückel model, indicating that π electronic effect is the key factor determining the relative stability of DA adducts. Based on these results, we propose a couple of simple rules of thumb, in terms of a set of bond patterns, as a visual guide for approximate prediction of DA reactive sites. Moreover, we suggest two quantitative descriptors for the stability of DA regioadducts of empty fullerenes; one combines the π free valences and bond orders involved in the DA addition, and the other characterizes the local π aromaticity around the addition site. The latter criterion allows us to easily rationalize the proposed rules.

Cycloaddition reactions play a preeminent role in the functionalization of fullerenes, enabling the preparation of a large variety of new derivatives with applications in material and biological sciences.[1–3] In particular, Diels–Alder (DA) reaction is a powerful tool for introducing a six-membered ring to the carbon cage.[1–3] Many DA adducts have been isolated and identified for empty fullerenes[4–6] and endohedral metallofullerenes (EMFs).[7–10]

Since there exist different types of C–C bonds on a fullerene cage, regioselectivity of DA additions is commonly exhibited. As the simplest example, C_{60} possesses two kinds of bonds, the more single-bond-like [5,6] and the more double-bond-like [6,6] types.[1] Experiments[4] and computations[11] indicate that, in the case of C_{60}, the cycloaddition to the more dienophilic [6,6] bond is distinctly preferred, both thermodynamically and kinetically. Larger and less symmetrical fullerenes, however, may have so many nonequivalent addition sites that the DA selectivity does not often follow this simple intuitive bond classification. For instance, among all 13 possible regioadducts of $C_{78}(5)$ with 1,3-butadiene (BD), the most stable one corresponds to a [5,6] adduct, as revealed by DFT calculations.[12,13]

To understand and predict the DA selectivity of fullerenes, various models as distortion/interaction[14–18] and criteria, based on arguments such as bond orders,[11] bond lengths, pyramidalization angles and HOMO–LUMO interactions,[12,14,15] have been commonly applied. However, there are no clear and universal rules that allow making reliable predictions of regioselectivity.[13] For instance, it is empirically suggested to combine the last three criteria to predict bond reactivity for the DA additions of BD with empty fullerene $C_{78}(5)$.[12]

Reaction energy (ΔE_R) is a relevant indicator of reactivity, especially for high-temperature synthesis. For many reactions, it is expected to follow the same trend as activation barrier, as implied by Hammond's postulate and Evans–Polanyi principle. In particular, for the DA additions to neutral fullerenes, we have confirmed the general correlation between ΔE_R and energy barriers for all systems considered in this study (see Fig. S1, ESI†). Therefore, although we will focus on the DA thermodynamic reactivity, many conclusions are also valid for the kinetic reactivity. Both are chiefly governed by the stabilization of the global π system when forming the adducts. This conclusion is borne out by the good agreement between the reaction energies obtained from sophisticated DFT computations and those from a simple model[19,20] based on the Hückel molecular orbital (HMO) theory (see the ESI† for computational details). This Hückel-based model has been recently implemented in the FullFun software package.[21] Requiring solely topological information, a HMO-based model has two advantages: it is almost

[a] *Departamento de Química, Universidad Autónoma de Madrid, Módulo 13, 28049 Madrid, Spain. E-mail: yang.wang@uam.es, manuel.alcami@uam.es*
[b] *Institute for Advanced Research in Chemical Sciences (IAdChem), Universidad Autónoma de Madrid, 28049 Madrid, Spain*
[c] *School of Chemistry and Chemical Engineering, Yangzhou University, Yangzhou, Jiangsu 225002, China*
[d] *Instituto Madrileño de Estudios Avanzados en Nanociencia (IMDEA-Nanociencia), 28049 Madrid, Spain*

† Electronic supplementary information (ESI) available: It includes correlations between ΔE_R and energy barriers, computational details, comparison between two dienes, correlations between DFT ΔE_R and XSI index for other fullerenes, general correlations, explicit illustrations of Fig. 1, and performance of CARI and ΣMCI for other fullerenes. See DOI: 10.1039/c8cc01709c

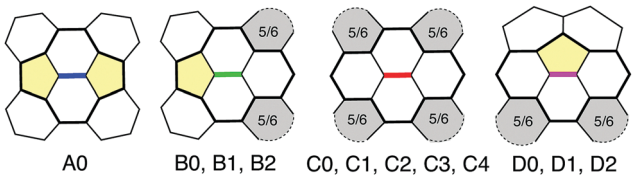

Fig. 1 All possible bond patterns in IPR fullerenes. Each pattern corresponds to a central bond highlighted by a thick line. In this notation, the preceding letter denotes the major type distinguished by the first layer of rings (with pentagons highlighted in yellow). The following number counts the pentagons in the second layer, defining the subtype of bonds. Some rings in the second layer with a '5/6' label (highlighted in grey) indicate that they can be either a pentagon or a hexagon.

costless in computer time for typical fullerenes, and therefore can be used as a predictive tool over huge families of compounds; it considers only π effects, allowing a much simpler interpretation. Using HMO-based parameters we have extensively studied the thermodynamic stability of DA regioadducts of neutral empty fullerenes ranging from C_{60} to C_{180}. For each cage size, we choose the lowest-energy isomer reported in the literature[22] that obeys the isolated pentagon rule (IPR).[23] By systematically analyzing the results, we propose a couple of simple rules of thumb, in terms of a set of bond patterns distinguished by their surrounding rings (see Fig. 1), as a visual guide to rapidly determine the DA reactivity of empty fullerenes. Although some previous studies used the major bond types in Fig. 1 to analyze the reactivity of some EMFs,[3,11–13] systematic correlation between bond patterns and stability of DA adducts has never been reported.

Our first goal is to reproduce by using HMO the ΔE_R of all possible adducts of a given cage obtained at DFT level. We have thus employed our recently developed exohedral fullerene stabilization index (XSI) model.[20] The model incorporates all three key factors responsible for the relative stability of exohedral fullerenes, namely, π delocalization over the cage, σ strain induced by fused pentagons, and steric hindrance among addends. In the particular case of DA adducts of IPR fullerenes, the strain effect is not present and the steric effect, which is approximately proportional to the number of adjacent addends, is identical for all isomers. This leaves us only the π stabilization term in the XSI to quantify the ΔE_R of DA adduct j of a given fullerene C_{2n}, as follows:

$$X_j = \sum_{k=1}^{n} \chi_k - \sum_{k=1}^{n-1} \chi_k^j \qquad (1)$$

where $\{\chi_k\}$ and $\{\chi_k^j\}$ are, respectively, the highest n and $(n-1)$ eigenvalues of the adjacency matrices associated with the empty cage C_{2n} and its j-th DA adduct. In the latter matrix, the rows and columns of the two carbon atoms on which the addition takes place are set to zero, and therefore removed. The relative energy of adduct j can thus be estimated as the value of X^j in units of -2β, with β being the resonance integral between carbons. A similar parameter evaluated on the diene was used by Houk *et al.* to predict the most reactive diene in DA reaction with C_{60}.[24] Note that the diene structure is not explicitly specified in the adjacency matrix of adduct. Nevertheless, our DFT calculations show very similar ΔE_R for dienes BD and cyclopentadiene (see ESI†).

Fig. 2 shows a nice correlation between X^j and the DFT ΔE_R for DA additions of BD to some typical fullerenes, *viz.*, C_{60}, C_{70}, $C_{76}(1)$ and $C_{84}(23)$. A general correlation for all these systems can be also obtained (see Fig. S12 in the ESI†). The correlations for other fullerenes, including non-IPR ones, are presented in

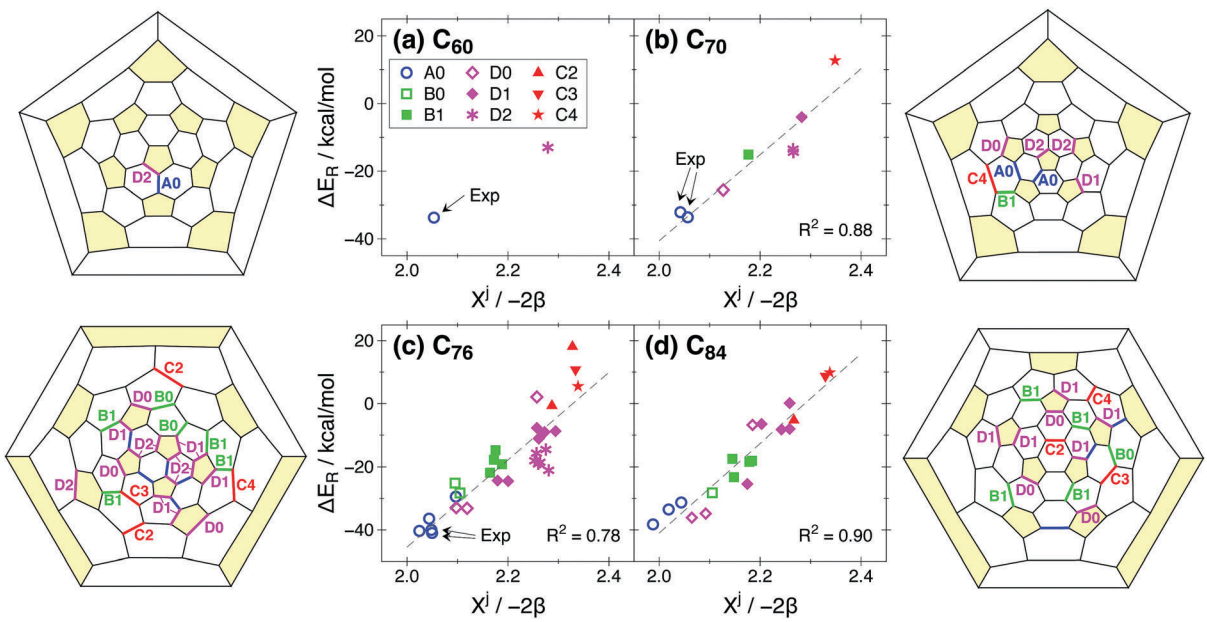

Fig. 2 Correlation between DFT reaction energies (ΔE_R) and π stabilization index (X^j) for DA additions of BD to (a) C_{60}, (b) C_{70}, (c) $C_{76}(1)$ and (d) $C_{84}(23)$. Correlation coefficients R^2 and experimental adducts[4–6] are indicated. In the Schlegel diagrams, all nonequivalent bonds are colored and labeled according to the bond patterns defined in Fig. 1. For C_{76} and C_{84} 'A0' labels for the blue bonds are omitted for clarity.

the ESI.† These results verify that the X^j is a reliable indicator of the DA ΔE_R of empty fullerenes and imply that the main factor accounting for DA reaction energy arises from π stabilization.

A remarkably interesting observation from Fig. 2 is that, in all cases, the site preference of DA addition strongly correlates with the bond types defined in Fig. 1. It is known that C–C bonds of an IPR fullerene can be classified into four major types, A–D (distinguished by different colors in Fig. 2), depending on the placement of pentagons and hexagons in the first surrounding layer.[3,11–13] Fig. 2 reveals that the bond reactivity of an IPR fullerene follows the overall trend: A > B ≈ D > C. All DA adducts of empty fullerenes C_{60}, C_{70} and C_{76} synthesized and unambiguously characterized to date[4–6] (labeled as Exp in Fig. 2), correspond to type A.

The major bond types can be further categorized into subtypes, based on how many pentagons (regardless of their positions) are present in the second peripheral layer (see Fig. 1). Specifically, 12 subtypes are possible for IPR fullerenes, *i.e.*, A0, B0–B2, C0–C4 and D0–D2, where the notation indicates firstly the major type followed by the number of pentagons in the second layer (see Fig. S11 in the ESI† for explicit illustrations). As shown in Fig. 2, for bonds of the same major type, the subtypes (displayed by the same color but different symbols) with fewer second-layer pentagons are generally more reactive.

As stated before, there have been many attempts to find an indicator that correlates with regioselectivity[25,26] but they show many exceptions.[13] We have explored several indicators that can be easily obtained from a single HMO calculation of the empty fullerene cage (instead of performing many calculations of X^j for all different regioadducts).

The best indicator we have found is what we call the cycloaddition reactivity index (CARI), defined as

$$\mathrm{CARI} = F_a + F_b - \sum_{i=1}^{5} B_i = 2\sqrt{3} - 2\sum_{i=1}^{5} B_i - B_1 \qquad (2)$$

where F_a and F_b are free valences of atoms a and b, and B_i are bond orders of the five surrounding bonds (Fig. 3a), evaluated by HMO theory (see ESI† for details).

The concepts of free valence and bond order were used in early works to study radical additions to fullerenes.[27,28] A direct interpretation of CARI is that it quantifies the ability of atoms a and b to form new bonds with the diene and the difficulty to break all π bonds involved in the addition. Alternatively, as indicated by the right-hand side of eqn (2) (obtained by using eqn (S2) in ESI†), CARI penalizes the loss of π bonds in the vicinity of the addition site with an extra weight on the central

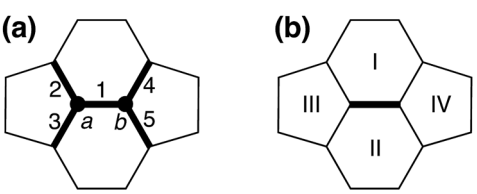

Fig. 3 Labeling of atoms, bonds and rings for defining the descriptors (a) CARI and (b) ΣMCI, exemplified by the A type bond.

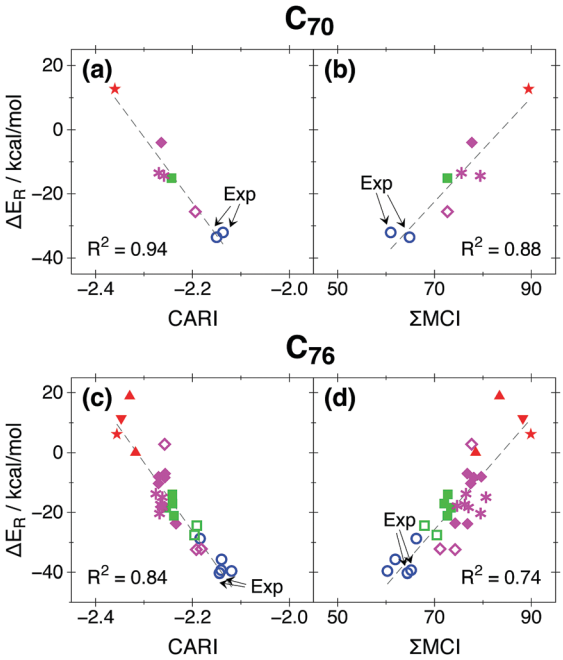

Fig. 4 Correlation between ΔE_R and two reactivity descriptors, CARI (a and c) and ΣMCI (b and d), for all DA adducts of C_{70} and C_{76}. Color and symbol codes are the same as in Fig. 2. Correlation coefficients R^2 and experimental adducts[4–6] are indicated.

one (*i.e.*, B_1). This implies that evaluation of addition reactivity based on the whole delocalization system can be approximated as a localized effect near the addition site. An excellent agreement is exhibited between ΔE_R and CARI for each cage (see Fig. 4a and c for C_{70} and C_{76}). Moreover, there exists a global correlation (ΔE_R = −206.8·CARI − 478.9 kcal mol^{-1}) for all different fullerenes (see Fig. S12 in the ESI†).

An extensive examination of IPR fullerenes of all sizes (up to C_{180}, see Fig. S13–S22 in the ESI†) also shows a correlation between X^j and CARI and further suggests that the systematic correlation between bond patterns and values of X^j described before is more the rule than the exception. This correlation could be used to roughly predict the thermodynamic stability of the corresponding DA adduct. For instance, for the most stable fullerenes smaller than C_{124}, the lower values of X^j clearly correspond to A0 adducts which are at least 0.05 (in units of -2β) lower than the X^j values for B0 and D0 adducts. C_{100} could be an exception since B0 and D0 adducts present values of X^j only 0.012 (in units of -2β, *ca.* 1.4 kcal mol^{-1}) higher than the lowest one. In this case, our DFT calculations show that the most stable structure for DA addition of BD to C_{100} corresponds to a D0 adduct. For larger fullerenes, A0 bonds do not appear or are scarce in the most stable cage. In these cases, B0 and D0 adducts have the lowest values of X^j.

Alternatively, we also see a strong connection between DA reactivity and local π aromaticity around the addition site. The latter can be evaluated, within HMO theory, as a sum of the multicenter indices (MCI)[29] of the four rings (I–IV, see Fig. 3b) surrounding the addition bond. Fig. 4b and d (Fig. S23 and S24 in the ESI† for other fullerenes) suggests that the more local

aromaticity (ΣMCI) around a bond, the less reactive it is. Local aromaticity has also been shown to play a key role in the selectivity of Bingel–Hirsch additions to EMFs.[30,31]

From aromaticity perspective, we can easily understand the above-proposed topological rules. Since pentagons are less aromatic than hexagons in neutral empty fullerenes,[30–32] major bond types containing more pentagons are less aromatic and therefore more reactive, explaining the first rule of DA reactivity order for IPR fullerenes: A > B ≈ D > C. As a secondary effect, the presence of pentagons in the second layer generally increases the aromaticity of the rings in the first layer.[33] Thus, bond subtypes with fewer second-layer pentagons are more reactive, as stated in the second rule.

In summary, inexpensive Hückel calculations can quantitatively predict DA reaction energies and provide simple reactivity descriptors based on bond order/free valence or aromaticity. These results allow us to establish simple topological rules to predict stable DA adducts and regioselectivity. Applying these models to EMF reactivities would be an interesting perspective, although charge transfer and metal-cage interactions[3,11–15] are additional effects not considered here.

This work was supported by the Spanish MINECO projects FIS2016-77889-R, CTQ2013-43698-P, CTQ2016-76061-P, the CAM project NANOFRONTMAG-CM (S2013/MIT-2850) and the European COST Action CM1204 XLIC. Calculations were performed at Centro de Computación Científica (CCC) of UAM. P. P. acknowledges the Spanish MECD for a FPU contract. Y. W. gratefully acknowledges the Thousand Talents Plan for Young Professionals of China.

Conflicts of interest

There are no conflicts to declare.

References

1 A. Hirsch and M. Brettreich, *Fullerenes: Chemistry and Reactions*, Wiley-VCH, Weinheim, Germany, 2005, pp. 101–183.
2 R. Caballero, P. de la Cruz and F. Langa, *Fullerenes: Principles and Applications*, The Royal Society of Chemistry, Cambridge, UK, 2nd edn, 2011, pp. 66–124.
3 A. Rodríguez-Fortea, S. Irle and J. M. Poblet, *Wiley Interdiscip. Rev.: Comput. Mol. Sci.*, 2011, **1**, 350–367.
4 Y. Rubin, S. Khan, D. I. Freedberg and C. Yeretzian, *J. Am. Chem. Soc.*, 1993, **115**, 344–345.
5 A. Herrmann, F. Diederich, C. Thilgen, H.-U. T. Meer and W. H. Müller, *Helv. Chim. Acta*, 1994, **77**, 1689–1706.
6 P. Seiler, A. Herrmann and F. Diederich, *Helv. Chim. Acta*, 1995, **78**, 344–354.
7 E. B. Iezzi, J. C. Duchamp, K. Harich, T. E. Glass, H. M. Lee, M. M. Olmstead, A. L. Balch and H. C. Dorn, *J. Am. Chem. Soc.*, 2002, **124**, 524–525.
8 H. M. Lee, M. M. Olmstead, E. Iezzi, J. C. Duchamp, H. C. Dorn and A. L. Balch, *J. Am. Chem. Soc.*, 2002, **124**, 3494–3495.
9 Y. Maeda, S. Sato, K. Inada, H. Nikawa, M. Yamada, N. Mizorogi, T. Hasegawa, T. Tsuchiya, T. Akasaka, T. Kato, Z. Slanina and S. Nagase, *Chem. – Eur. J.*, 2010, **16**, 2193–2197.
10 S. Sato, Y. Maeda, J.-D. Guo, M. Yamada, N. Mizorogi, S. Nagase and T. Akasaka, *J. Am. Chem. Soc.*, 2013, **135**, 5582–5587.
11 J. M. Campanera, C. Bo and J. M. Poblet, *J. Org. Chem.*, 2006, **71**, 46–54.
12 S. Osuna, M. Swart, J. M. Campanera, J. M. Poblet and M. Solà, *J. Am. Chem. Soc.*, 2008, **130**, 6206–6214.
13 S. Osuna, M. Swart and M. Solà, *Phys. Chem. Chem. Phys.*, 2011, **13**, 3585–3603.
14 F. M. Bickelhaupt, M. Solà and I. Fernández, *Chem. – Eur. J.*, 2015, **21**, 5760–5768.
15 Y. García-Rodeja, M. Solà, F. M. Bickelhaupt and I. Fernández, *Chem. – Eur. J.*, 2017, **23**, 11030–11036.
16 C.-X. Cui and Y.-J. Liu, *J. Phys. Chem. A*, 2015, **119**, 3098–3106.
17 C.-X. Cui, Y.-J. Liu, Y.-P. Zhang, L.-B. Qu and Z.-P. Zhang, *J. Phys. Chem. A*, 2017, **121**, 523–531.
18 C.-X. Cui, Z.-P. Zhang, L. Zhu, L.-B. Qu, Y.-P. Zhang and Y. Lan, *Phys. Chem. Chem. Phys.*, 2017, **19**, 30393–30401.
19 Y. Wang, S. Díaz-Tendero, M. Alcamí and F. Martín, *Nat. Chem.*, 2015, **7**, 927–934.
20 Y. Wang, S. Díaz-Tendero, M. Alcamí and F. Martín, *J. Am. Chem. Soc.*, 2017, **139**, 1609–1617.
21 Y. Wang, S. Díaz-Tendero, M. Alcamí and F. Martín, *J. Chem. Theory Comput.*, 2018, **14**, 1791–1810.
22 Y. Wang, S. Díaz-Tendero, M. Alcamí and F. Martín, *Phys. Chem. Chem. Phys.*, 2017, **19**, 19646–19655.
23 H. W. Kroto, *Nature*, 1987, **329**, 529–531.
24 Y. Cao, Y. Liang, L. Zhang, S. Osuna, A.-L. M. Hoyt, A. L. Briseno and K. N. Houk, *J. Am. Chem. Soc.*, 2014, **136**, 10743–10751.
25 S. Osuna, M. Swart and M. Solà, *J. Am. Chem. Soc.*, 2009, **131**, 129–139.
26 T. Yang, X. Zhao, S. Nagase and T. Akasaka, *Chem. – Asian J.*, 2014, **9**, 2604–2611.
27 K. M. Rogers and P. W. Fowler, *Chem. Commun.*, 1999, 2357–2358.
28 B. de La Vaissiere, J. P. B. Sandall, P. W. Fowler, P. de Oliveira and R. V. Bensasson, *J. Chem. Soc., Perkin Trans. 2*, 2001, 821–823.
29 P. Bultinck, R. Ponec and S. Van Damme, *J. Phys. Org. Chem.*, 2005, **18**, 706–718.
30 M. Garcia-Borràs, M. R. Cerón, S. Osuna, M. Izquierdo, J. M. Luis, L. Echegoyen and M. Solà, *Angew. Chem., Int. Ed.*, 2016, **55**, 2374–2377.
31 M. Garcia-Borràs, S. Osuna, J. M. Luis, M. Swart and M. Solà, *Chem. Soc. Rev.*, 2014, **43**, 5089–5105.
32 M. Garcia-Borràs, S. Osuna, M. Swart, J. M. Luis and M. Solà, *Chem. Commun.*, 2013, **49**, 1220–1222.
33 G. Van Lier, P. W. Fowler, F. De Proft and P. Geerlings, *J. Phys. Chem. A*, 2002, **106**, 5128–5135.